FINAL REPORT
GRANT NGR-34-002-038
June 30, 1969

"A STUDY OF OPTICAL DATA PROCESSING AND REDUCTION"

to
ational Aeronautics & Space Administration
Washington, D. C.

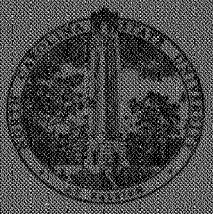

DEPARTMENT OF ELECTRICAL ENGINEERING
NORTH CAROLINA STATE UNIVERSITY
RALEIGH, NORTH CAROLINA

FINAL REPORT
GRANT NGR-34-002-038
June 30, 1969

"A STUDY OF OPTICAL DATA PROCESSING AND REDUCTION"

to
National Aeronautics & Space Administration
Washington, D. C.

North Carolina State University
Raleigh, North Carolina

Submitted: F. J. Tischer

Dr. F. J. Tischer, Professor
Principal Investigator

TABLE OF CONTENTS

INTRODUCTION

This is the final report on Grant NGR-34-002-038. It presents a review of the activities, of the research carried out under the grant, and of the results. It also contains a report on the results of research carried out under a no-cost extension during the period July 1, 1968, to March 31, 1969, when the grant was terminated. The original grant period was July 1, 1966, to June 30, 1968. During this period, the results of the research were presented by progress reports.

One of the objectives of the activities under the grant was to assist the National Aeronautics and Space Administration in its operations of applying optical methods for data and information handling. This assistance was given by carrying out literature searches, by the initiation of short courses on optical data processing available to NASA personnel, by carrying out specific studies, by research related to pertinent optical processing methods, such as correlation processing, and by developing new methods of analysis and measurement of related optical phenomena. The cooperation with the Space Data Control Branch, Code 521 of GSFC, and the many stimulating discussions with Mr. Arnold Schulman are highly appreciated.

The research was carried out by the principal investigator assisted by graduate and undergraduate students. The names of the students working on specific projects were listed in the progress reports. One of the students, Dr. J. P. Moffatt, completed his dissertation entitled "Effects of Geometric Deviations

and Nonlinearities in Coherent Optical Data Processors" in May 1968 on research under the grant.

RESEARCH REVIEW

The research started with specific problems related to the detection of signals in noise by optical correlation processing. Various types of errors which limit the efficiency of the optical approach in comparison with electronic methods were investigated. The effects of the DC-stop, of finite dimensions of the optical signal and filter distributions, and of the nonlinearities were studied. Attempts were then made to find methods for the elimination or reduction of these effects. A typical example is a function linearizer which is a device to be inserted between an electronic signal source and an optical signal recorder and which introduces additional nonlinearities such that they compensate the original ones. A prototype model of such a device was fabricated and operated satisfactorily for compensating the nonlinear effects of cathode ray tubes at optical signal recording. On the side of this initial research a bibliography of books and articles dealing with optical data processing was prepared and published.

Correlation and spectrum analysis of holograms is another subject matter which attracted the interest of students as a dissertation topic. Such correlation methods are important since they may increase the capabilities of holographic computer memories, may be used for three-dimensional-character and body recognition, for rendevous-guidance of space vehicles, and for the determination of the orientation of various types of bodies. A number of elementary steps of the investigation was completed

during the grant period. The results were presented in three progress reports.

The study of errors of optical data processors raised the question of how to define numerically the quality of the great variety of such devices and methods. Study of the literature and discussions led to adopting a noise-to-signal ratio as a characteristic quantity. By considering the deviation of the actual optical signal from the hypothetical signal obtained under ideal conditions as noise and relating it to the undisturbed signal intensity, such a quantity, which is customarily used in electronic data processing, can also be formulated for optical signals and their processing.

By the use of the noise-to-signal ratio, investigations were then carried out to optimize dimensions and operational conditions of elements of optical data processors. Tolerances of the dimensions and geometries of such elements for keeping the quality of data processing above specified levels were formulated and found. The results of these studies form a part of Mr. Moffatt's dissertation.

Considerable efforts were made to find a new method for the description of nonlinear effects, since previously used methods are inaccurate and difficult to apply as shown in a comparitive study. Use of Chebyshev polynomials led to a satisfactory solution. The new method is particularly well-suited for optical data processing and holography since the signals are mostly sinusoidal in these operations or can be represented by such a signal form.

An advantageous feature of representing nonlinear char-cteristics by Chebyshev series is the fact that expreiments can be designed to check the theoretical results, to find experimentally the characteristics of various devices, and to describe them with satisfactory accuracy.

Based on these theories, computer programs were developed for the evaluation of the characteristics of photographic plates and film, such as spectroscopic plates 649-F, and diagrams made which show the effects of nonlinearities of signals recorded on such plates. Another program gives the noise-to-signal ratio as a function of the bias illumination and the recorded signal amplitude. The resulting noise-to-signal ratios presented in diagram form indicate the optimum bias levels for obtaining minimum distortions. The theoretical and computed results were checked by experiments and were found in satisfactory agreement. The results were presented at meetings of the Optical Society of America and found considerable interest indicated by the large number of requests for reprints.

During the no-cost extension, research carried out at a reduced level of efforts dealt with a study of nonlinear effects on holography. It was found that nonlinearities result in secondary or "ghost" images. The theory and an experimental verification of these effects is presented in this report.

LIST OF INVESTIGATED RESEARCH TOPICS

1. Preparation of "Bibliography on Optical Information and Data Processing" (November 1966)
2. Effect of the finite width of a DC-stop filter
3. Nonlinear effects in correlation processing
4. Methods for the compensation of nonlinear effects in optical recording and readout
5. Effects of the finite width of optical signals and filters
6. Correlation and spectrum analysis of holograms
7. Effects of the shape of carrier surfaces on optical data processing
8. Unified theory of diffraction
9. Measurement of the permeability of magnetic fluids
10. New methods in considering nonlinear effects in optical data processing
11. Representation of optical errors by noise-to-signal ratios
12. Nonlinear effects in holography

SEMINARS, CONFERENCES, AND PUBLICATIONS

1. Attendance of a short course entitled "Introduction to Optical Data Processing," University of Michigan, Ann Arbor, Michigan, July 25 to August 5, 1966.
2. Participation at "Symposium on Modern Optics," Brooklyn Inst. of Techn., New York, March 22-24, 1967. Presented paper: "Schlieren Prism." (Co-author, A. T. Shankle).
3. Preparation and presentation of a short course on "Mathematical Fundamentals of Optical Wave Propagation" at NASA-GSFC, Greenbelt, Maryland, June 26 to June 30, 1967.
4. Preparation and presentation of a short course with computation sessions on Optical Wave Propagation" NASA-GSFC, Greenbelt, Maryland, September 28 to October 4, 1967.
5. Spring Meeting, Optical Society of America, Washington, D. C., March 13-16, 1968. Presented paper: "Nonlinear Optical Recording in Data Processing and Holography." (J. P. Moffatt and F. J. Tischer) "Unified Theoretical Formulation of Electromagnetic Diffraction." (F. J. Tischer)
6. Publication entitled, "Schlieren Prism for Light Beams" A. T. Shankle and F. J. Tischer in "Modern Optics" Polytechnic Press, Vol. XVII, 257-264.
7. Annual Meeting, Optical Soc. of Am., Pittsburgh, Pa., October 9-11, 1968. Presented paper: "Measurement of Nonlinear Effects at Optical Recording." (F. J. Tischer)

8. Spring Meeting, Optical Soc. of Am., San Diego, Calif., March 11-14, 1969. Presented paper: "Analysis of Non-linear Effects in Holography by Chebyshev Polynomials." (F. J. Tischer)

LIST OF REPORTS

The Effect of Finite Width of the DC-Stop in Optical Correlators
(Preliminary results, 11 pages) August 1966)

Bibliography on Optical Information and Data Processing
(Listing of books and articles, 73 pages) November 1966

The Effect of Non-Linearities on Optical Correlation Processing
(Preliminary results, 17 pages) November 1966

Progress Report (July 1 to December 31, 1966) January 1967
Subtitles: "The Effects of Finite Spatial Distributions and Time Response in Optical Recording."
"Correlation Analysis of Holograms - General Relationships"

Progress Report (January 1 to April 30, 1967) May 1967
Subtitles: "Nonlinear Function Modifier"
"Effects of Shape of Signal Carrier Surfaces in Optical Data Processing"
"Correlation Processing of Holograms - Auto-correlation Processing"

Progress Report, July 1967
(Summaries, work in progress, and plans)

Progress Report (July 1 to September 15, 1967) September 1967
Subtitles: "Consideration of Nonlinear Effects by Chebyshev Polynomials"
"Expression of the Effects of the Non-linearities by a Signal-to-Noise Ratio"
"Nonlinear Effects in Optical Correlation - Continuation"

Progress Report (September 15 to December 15, 1967) 30 pages, December 15, 1967

Subtitles: "A Unified Theoretical Formulation of Electromagnetic Diffraction"
"Nonlinear Effects in Optical Processes - Continuation"
"Measurement of the Permeability of a Ferro-Magnetic Fluid"
"Correlation Processing of Holograms - Comparison with Spectrum Analysis"

Progress Report (January 1 to March 31, 1968) March , 1968

Subtitle: "Final Report on Nonlinear Effects in Optical Data Processing"

Final Report (Period ending June 30, 1968, 161 pages) June 1968

Subtitle: "Effects of Geometric Deviations and Non-linearities in Coherent Optical Data Processors"

ANALYSIS OF "GHOST" IMAGES IN HOLOGRAPHY BY CHEBYSHEV POLYNOMIALS

Abstract

Nonlinear effects in holography resulting in "ghost" images at the reconstruction are studied by the use of Chebyshev polynomials. Equations are derived for the transmittance of off-axis holograms and for the reconstructed images for the two-dimensional case. Using Chebyshev series, the equations become relatively simple in the case of line and point objects since the various terms of the series represent corresponding pairs of the images, of the linear images and of the ghost images caused by nonlinearities. Light powers transmitted by the various beams can be computed and noise-to-signal ratios defined as figures of merit for the holographic processes and for the used recording materials. Optimum light levels of the reference and signal beams can be found. Experiments are described which confirm the validity of the concepts and of the computed relationships.

Introduction

Quality and efficiency of operations in optical data and image processing are often degraded by nonlinear effects. Such effects are primarily encountered in recording and read-out, but also in other operations in optical systems. Holography which is an optical recording process is a typical example. It is strongly affected by nonlinearities. The consequences of the nonlinearities are ghost images which are observed at the reconstruction.

The nonlinear relationship in photographic recording can be observed at inspecting the characteristic curve for photographic material which relates the local amplitude transmittance of a photographic plate or film as the output quantity to the exposure as the input quantity. This diagram is more useful from a viewpoint of reconstructing holographic images, than the customarily used H & D curve for photographic processing which interrelates density and logarithmic exposure. If the former relationship were represented by a straight line, higher order derivatives being zero, no nonlinear effects would occur and the reconstructed image would be identical to the original object, disregarding other undesired side effects. This, however, is not the case and, depending on the point of operation on the characteristic T & E (transmittance versus exposure) curve, a varying amount of nonlinear distortions is present which result in undesired secondary or "ghost" images at the reconstruction.

Nonlinear effects in holography have been investigated by several authors[1-6], however, the derived equations are of considerable complexity since they usually include multiple correlation integrals[5] - also for simple objects. It then becomes difficult to derive a clear understanding of the equations and to give a physical interpretation of the relationships between the various quantities. It is the purpose of this paper to outline a new method of representation and evaluation of nonlinear effects in holography. The method leads to comparatively simple relationships particularly at the consideration of rather basic object configurations such as lines and points. The resulting relationships can be readily interpreted and instructively show the origin and optical background of the nonlinear holographic phenomena. They also permit finding optimum operational conditions for keeping these effects small.

The new method is based on describing nonlinear relationships between input and output quantities of optical processes by Chebyshev polynomials. The figures which describe the form of the relationship are the coefficients of a Chebyshev series. This approach replaces the usually used methods of representing the characteristic relationship by Taylor series, Fourier relationships, and gamma-coefficient models. The use of Chebyshev polynomials in holography seems to be particularly advantageous in the case of simple objects. The ghost images resulting from nonlinearities are then simple described by one Chebyshev coefficient each. In contrast to that, infinite series of coefficients and integrals are required for

the description of each image if one of the other known methods is used. The described procedure also offers the possibility of defining the characteristics of ghost images by individual noise-to-signal power ratios and the over-all quality of the imaging process by a total noise-to-signal ratio. These quantities can be computed from the T & E curve of the holographic plate. Experiments based on these considerations have confirmed the basic concepts and accurate numerical studies of nonlinear effects are possible.

Method of Analysis

It is known that an arbitrary continuous relationship between two quantities can be described for a finite interval by Chebyshev polynomials. A variable u_1 is assumed which, between its values -1 and +1, represents the finite interval of the input quantity. The output quantity u_2 can then be expressed by

$$u_2 = f(u_1) = \frac{1}{2} b_o + \sum_{n=1}^{\infty} b_n T_n(u_1) \quad , \tag{1}$$

where the functions $T_n(u_1)$ are the Chebyshev polynomials which are orthogonal and where the coefficients are given by

$$b_n = \frac{2}{\pi} \int_{-1}^{+1} f(u_1) \, T_n(u_1) \, \frac{du_1}{1 - u_1^2} \quad . \tag{2}$$

The Chebyshev series has interesting features if the input quantity varies sinusoidally according to $u_1 = \cos wx$. Since the terms of the Chebyshev series can be written alternatively as

$$T_n(u_1) = \cos (n \cos^{-1} u_1) \quad , \tag{3}$$

one finds

$$T_n(u_1) = \cos nwx \quad , \tag{4}$$

and the output quantity becomes as function of the variable x

$$u_2(x) = \frac{1}{2} b_o + \sum_{n=1}^{\infty} b_n \cos nwx \quad . \tag{5}$$

The output function is hence a Fourier series with the coefficients equal to those of the Chebyshev series. The first-order term with the coefficient b_1 has the same form as the

input function. The higher-order terms are harmonics caused by the nonlinearity of the function $f(u_1)$.

It is noteworthy that these conditions of a sinusoidally varying input quantity are exactly those encountered in holographic processes where interference pattern with such a distribution of the light intensity are recorded on the hologram. The description by Chebyshev polynomials seems thus ideally suited for holographic processing. The input quantity u_1 represents the varying part of the exposure E which varies sinusoidally around a bias value E_o as a function of the position on the plate described by x for a one-dimensional diffraction pattern. The output quantity u_2 stands for the deviation of the transmittance from its value for $u_1 = 0$.

Characteristics of Holographic Plates

The characteristics of a photographic plate or film for holography can be best described by the T & E curves. Examples are shown in Fig. 1 for spectroscopic plates 649-F of Kodak, which are derived from D and logE curves published by the company. The curves can be evaluated by a computer program[7] which yields the Chebyshev coefficients according to Eq. (2). The coefficients are computed in terms of two quantities. One is the bias exposure E_b which is proportional to the light intensity I_b of the reference beam ($E_b = I_b t$, t = exposure time) in the absence of a signal beam. The other quantity is the amplitude of the sinusoidal variation of the exposure E_a due to interference with the signal beam. It should be noted that E_a is smaller

than E_b to satisfy the condition that E(x) remains positive. The distribution of the exposure is then for a one-dimensional interference pattern described by

$$E(x) = E_b + E_a \cos w_x x \quad . \tag{6}$$

The output quantity is the transmittance $\tau(x) = u_2(x)$ which is given by the right-hand side of Eq. (5). The coefficients b_n are now functions of the bias exposure E_b and the exposure amplitude E_a ,

$$b_n = F_n(E_b, E_a) \quad . \tag{7}$$

Figure 2 shows as an example a diagram for the first order term b_1 which also may be considered as the product of the input amplitude and the average slope of the characteristic curve. In the absence of nonlinearities, this term indicates the transfer characteristics of the holographic plate. Diagrams similar to those shown in Fig. 2 are obtained for the higher-order coefficients. If a hologram is illuminated, the higher-order terms are related to ghost images where each term of the Chebyshev series describes a pair of these, one real and one virtual image.

Diagrams for the Chebyshev coefficients as shown in Fig. 2 indicate thus minimum and maximum values of these coefficients as a function of the bias exposure and the amplitude of the sinusoidal variation and give an indication of the strength of the holographic ghost images. Such diagrams may hence be used for the numerical description of the properties of plates and films for making holograms. The diagrams can also be used for finding

optimum light-intensity levels of the reference beam when distortions by ghost images are a minimum.

An alternative method of describing the quality of holographic processes and of plates and films for holography can be derived from the concept to consider ghost images as optical noise in analogy to similar terms in electronic communications. Based on this concept, each ghost image can be described by a noise-to-signal power ratio (NSR) which represents the ratio of the light power transmitted to form this image divided by the power to form the image of the original object. In the case of holograms of basic objects such as planes and lines this ratio (NSR) simply becomes the ratio of the respective higher-order Chebyshev coefficient to the first-order coefficient squared. The noise-to-signal ratio of the nth-order ghost is hence

$$NSR_n = (b_n/b_1)^2 \quad .$$

A more general figure is found by adding the relative light powers transmitted to form all higher-order ghost images, where

$$NSR_{total} = \left(\sum_{n=2}^{\infty} b_n^2\right)/b_1^2 \quad .$$

It seems that this concept facilitates useful comparisons and numerical descriptions of processes and materials for holography.

Theory of Nonlinear Holography

Based on the preceding equations, relationships can be derived for the theoretical description of holographic recording. The conditions and the geometry which are the basis of the

derivation are shown in Fig. 3. A transmitting-type object is illuminated by a coherent, quasimonochromatic, and collimated light beam. The output beam represents the signal beam which, in the plane of the holographic plate, has an amplitude distribution

$$u(x,y) = a(x,y)e^{j\phi(x,y)} \quad . \tag{8}$$

The reference beam has a distribution at the same location given by $\exp(jw_x x)$, assuming that its transverse amplitude distribution is constant and normalized to unity. The total exposure at the plate is then proportional to the total absolute value squared

$$E(x,y) = \left|\exp jk_x x + a(x,y)\exp[j\phi(x,y)]\right|^2 \tag{9}$$

Evaluation yields

$$E(x,y) = \underbrace{1 + a^2(x,y)}_{E_b(x,y)} + \underbrace{2a(x,y)}_{E_a(x,y)} \cos \underbrace{[k_x x - \phi(x,y)]}_{\psi(x,y)} \quad , \tag{10}$$

and in simplified writing

$$E(x,y) = E_b(x,y) + E_a(x,y) \cos \psi(x,y) \quad . \tag{11}$$

The functions E_b and E_a vary slowly as a function of x and y, while cos ψ varies fast. The separation of E(x,y) into parts varying slowly and fast with position contains an element of arbitrariness but it is justified in the case of off-axis holography. In this case the conditions are similar to those in electronic modulation theory where similar representations are used for modulated-carrier signals.[8]

With reference to Eq. (5), the transmittance resulting from the photographic process becomes a linear superposition of terms

$$\tau(x,y) = \tau_o(x,y) + \sum_{n=1}^{\infty} \tau_n(x,y) \quad , \tag{12}$$

where the various terms are given by

$$\tau_o(-x,y) = \tau_{oo}[E_b(x,y)] + \frac{1}{2} b_o[E_b(x,y), E_a(x,y)] \quad ,$$

$$\tau_n(x,y) = b_n[E_b x,y), E_a(x,y)] \cos n\psi(x,y) \quad . \tag{13}$$

It is noted that the Chebyshev coefficients b_n are functions of E_b and E_a which in turn are functions of x and y (slowly varying). They represent the envelopes of the rapidly oscillating functions $\cos n\psi(x,y)$ and can be obtained from diagrams such as shown in Fig. (2) or from the computer program. Reconstruction of the first-order term $\tau_1(x,y)$ yields the image of the original object, the reproducable real image and the observable virtual image. The higher-order terms of τ cause pairs of ghost images with beams linearly superimposed. Since the coefficients b_n are functions of x and y, they may be represented by Fourier series of the form

$$b_n(x,y) = \sum_o \sum_p c_{nop} \cos(ow_x x + p\omega_y y) \quad . \tag{14}$$

It is observed, taking into consideration Eq. (14), that the resulting equations become rather complex in the case of more complicated objects, leading to expressions of infinite series of multiple integrals.

Hologram of a Line Object

The equations presented in the preceding section become more useful if they are applied to simple objects such as a line object. The problem becomes then one-dimensional and the relationships can be readily interpreted and verified by experiments. The signal beam originating at the line source consists of cylindrical waves which give in the plane of the holographic plate a wave amplitude

$$W_1 = \frac{A_1}{\sqrt{D_1^2 + x^2}} \exp(jk_o \sqrt{D_1^2 + x^2}) \quad , \tag{15}$$

where A_1 is proportional to the amplitude of the line source and k_o is the free-space wave number or plane-wave propagation constant. Disregarding the small amplitude variation due the term in the denominator, the equation can be written as

$$W_1 = A_1 \exp \{jk_o D_1 [\sqrt{1 + (x/D_1)^2} - 1]\} \quad , \tag{16}$$

where the redefined A_1 represents now the amplitude in the sub-zenith point of the hologram plane where the origin of the coordinate system is located as indicated in Fig. 4a. The wave amplitude of the reference beam along the plate is

$$W_2 = A_2 \exp(jk_o x \sin\beta) \quad , \tag{17}$$

under the assumption that the beam hits the plate under an angle β against the plate normal and that A_2 is the amplitude at the origin.

Computation of the intensity of the interference pattern according to $I(x) = (W_1 + W_2)(W_1^* + W_2^*)$ yields

$$I(x) = 2A_1^2[1 + a^2 + a \cos \psi(x)] \quad , \tag{18}$$

where

$$a = A_2/A_1 \; ; \; \angle A_1 = \angle A_2 \quad ,$$

$$\psi(x) \simeq \frac{1}{2} k_o(x^2/D_1) - k_x x \; ; \; k_x = k_o \sin \beta \quad .$$

It is noted that Eq. (18) basically is the description of a one-dimensional interference pattern with a spatial wave number or phase constant in the x direction given by $d\psi(x)/dx$ which is

$$k_x(x) = d\psi(x)/dx = k_o x/D_1 - k_o \sin\beta \; .^*$$

Application of Eq. (11) gives the distribution of the exposure along the holographic plate

$$E(x) = E_b + E(a) \cos \psi(x) \quad . \tag{19}$$

The bias level which defines the point of operation along the T & E curve is $E_b = A_1^2 \, t(1 + a^2)$ and is constant. The amplitude of the sinusoidal variation of the exposure $E_a = A_1 \, t \, a$ is constant also. The phase term is given by Eq. (18)

$$\psi(x) = \frac{1}{2} k_o x^2/D_1 - k_o \, x \sin\beta \quad . \tag{20}$$

After exposing the plate according to Eq. (20), and processing it, the distribution of the resulting amplitude transmittance is given by

---

* It should be noted that the phase constants in the various directions of the local coordinate system are related by $k_x^2 + k_y^2 + k_z^2 = k_o^2$.

$$\tau(x) = \tau_o + \sum_{n=1}^{\infty} \tau_n(x) \quad , \tag{21}$$

where

$$\tau_o = \tau_{oo}(E_b) + \frac{1}{2} b_o(E_b,E_a) \quad ,$$

$$\tau_1 = b_1(E_b,E_a) \cos \psi(x) \; ; \; \tau_n = b_n(E_b,E_a) \cos n\psi(x) \; . \tag{22}$$

The Chebyshev coefficients b_n are now constants* and are independent of the position on the plate. The first order term yields the images of the line object if the plate is illuminated by coherent light. The higher-order terms $\tau_n(n>1)$ cause ghost images, each term of the Chebyshev series one pair of them. It is observed that simple relationships are obtained for the line object since each term of the Chebyshev series represents one pair of ghost images, one real and one virtual image. This is in contrast to other methods of representing nonlinear effects such as Taylor series where infinite series are obtained for the description of each ghost image.

General Image Reconstruction

In considering reconstruction of holograms containing nonlinearities, Fresnel imaging will be discussed only since Frauenhofer imaging seems to be of minor importance.** If the amplitude distribution of light leaving the hologram is $u_1(x_1,y_1)$,

---

* This is an approximation due to disregard of the term in the denominator of Eq. (15).

** Assuming a hologram size of 2.5 cm squared and a $\lambda/4$ criterion, the distance between the image plane and the hologram for Frauenhofer imaging is 4KM (2.5 miles).

the distribution in the image plane at a distance D_2 is obtained by the modified Fresnel-Kirchhoff diffraction formula[9] in customary notation

$$u_2(x_2,y_2) = K\iint_{Ap} u_1(x_1,y_1)G(x_2 - x_1, y_2 - y_1)dx_1dy_1 \quad , \tag{23}$$

$$K = -j\,\frac{4\pi}{\lambda}\cos\theta \quad ,$$

$$G = \frac{1}{4\pi}\,\frac{\exp(-jk_o r)}{r} \quad ; \quad r = \sqrt{D_2^2 + (x_2 - x_1)^2 + (y_2 - y_1)^2} \quad ,$$

where θ is the angle under which the illuminating light hits the hologram and G is the Green's function for free space.

The light amplitude in the output plane of the hologram is proportional to the transmittance and given by

$$u_1(x_1,y_1) = A_o\,\tau(x_1,y_1) = A_o \sum_{n=0}^{\infty} \tau_n(x_1,y_2) \quad , \tag{24}$$

with τ representing the transmittance distribution of the hologram and where A_o is the illuminating light amplitude. The various terms of the transmittance are obtained from Eq. (13), where the nth term has the form

$$\tau_n(x_1,y_1) = \frac{1}{2}\,b_n(x_1,y_1)\left[e^{jn\psi(x_1,y_2)} + e^{-jn\psi(x_1,y_2)}\right] \quad . \tag{25}$$

The two terms between the brackets describe phase variations of the hologram which under illumination cause the pair of real and virtual images of the nth order. Different terms may cause linearly superimposed light beams and images if they hit the imaging plane at the same place. The zero-order term represents an image of the slowly varying amplitude-envelope distribution of the hologram,

$$u_{20}(x_2,y_2) \simeq K_o\, b_o\,(x_1,y_1) \quad . \tag{26}$$

The first-order term describes the original object,

$$u_{21}(x_2,y_2) = K_1 \iint_{Ap} b_1(x_1,y_1)\exp[j\psi(x_1,y_1)]G(x_2-x_1,y_2-y_1)\,dx_1dy_1 \ , \tag{27}$$

and the ghost images are given by the higher-order terms

$$u_{2n}(x_2,y_2)K_n \iint_{Ap} b_n(x_1,y_1)\exp[jn\psi(x_1,y_1)]G(x_2-x_1,y_2-y_1)\,dx_1dy_1 \tag{28}$$

Reconstruction of the Line Image

The general relationships of the preceding section are applied next to the case of a line object discussed before. Under these conditions, the problem becomes one-dimensional and the equations can be readily evaluated. Assuming the obliquity factor to be unity and disregarding the variations of the distance r in the denominator of the Green's function ($r \simeq D_2$), Eq. (23) becomes

$$u_2(x_2) = -j\,\frac{e^{-jk_oD_2}}{\lambda D_2}\; e^{-j\frac{k_ox_2^2}{2D_2}} \int_{Ap} u_1(x_1)\, e^{j\frac{k_o}{2D_2}(x_1^2-2x_1x_2)}\,dx_1 \ . \tag{29}$$

The amplitude distribution according to Eq. (24) is now given by

$$u_1(x_1) = A_o \sum_{n=0}^{\infty} \tau_n(x_1) \quad , \tag{30}$$

where

$$\tau_n(x_1) = b_n(E_b,E_a)[e^{jn\psi(x_1)} + e^{-jn\psi(x_1)}] \quad , \tag{31}$$

and

$$\psi(x_1) = \frac{1}{2} k_o x_1^2/D_1 - k_o x \sin\beta \quad . \tag{32}$$

For the line object, the Chebyshev coefficients are constants which depend on the bias exposure E_b and on the amplitude of the cylindrical-wave signal beam E_a as indicated in Eq. (22). The phase term according to Eq. (32) is typical for a one-dimensional interference pattern with a linearly increasing phase constant (spatial frequency)

$$k_x = \frac{d\psi(x)}{dx} = k_o x_1/D_1 - k_o \sin\beta \quad .$$

Considering only the second phase term between the brackets of Eq. (31) which yields the real image, one obtains for the nth term of the reconstructed image

$$u_{2n}(x_2) = K_n b_n \int_{Ap} e^{j\frac{k_o}{2D_2}(x_1^2 - 2x_1x_2)} e^{-jk_o n\frac{x_1^2}{2D_1}} e^{jk_o n x_1 \sin\beta} dx_1 \quad . \tag{33}$$

Evaluation of the integral for the real image of the original object (n = 1) gives under the condition $D_1 = D_2 = D$

$$u_{21}(x_2) = K_1 b_1 \int_{Ap} e^{j(k_o \sin\beta - \frac{k_o}{D} x_2)x_1} dx_1 \quad . \tag{34}$$

The condition $D_2 = D_1$ implies that the distance between image plane and hologram at reconstruction equals that between line object and holographic plate when the hologram was made. Further evaluation yields

$$u_{21}(x_2) \simeq K\delta\left(k_o \sin\beta - \frac{k_o}{D} x_2\right) \quad . \tag{35}$$

The result is a δ-function at the position

$$x_2 = D \sin \beta \tag{36}$$

which represents the image of the original line source.

Evaluation of Eq. (33) for higher-order values of n shows that the ghost images are represented by δ-functions also, which are obtained for positions given by

$$D_2 = D_1/n \tag{37}$$

and at a transverse distance from the axis

$$x_2 = n\, D_2 \sin\beta = D \sin\beta \quad . \tag{38}$$

The results indicate that the ghost images of the line source occur at equal transverse positions x_2 but at different longitudinal positions D_2. Each Chebyshev coefficient and term of the series for τ describes one of them.

EXPERIMENTS

A series of experiments has been carried out to verify the derived relationships and to aid at their interpretation. Holograms were made of a line object and a point object since the described method of analysis is well suited for the study of simple objects. The experimental results verify the derived equations.

Experimental Setup

A major component of the experimental setup, which is illustrated in Fig. 4a, is a HeNe laser with a beam-expanding telescope which gives a collimated filtered beam. The beam is

divided by a beam splitter into two parts of which one passes through a cylindrical lens which focuses the beam along a line. The beam behind the focal region represents the signal beam which has characteristics similar to those of a beam caused by a line object. The second part of the beam travels straight through the beam splitter and passes through an attenuator. It is subsequently reflected by a mirror, and becomes the reference beam. Both superimposed beams form an interference pattern which is photographed on a Kodak 649-F plate. The photograph represents then an off-axis hologram of a line source. The distance between the focus of the cylindrical lens and the plate is D_1 and the angle under which the reference beam hits the plate is β.

Reconstruction is indicated in Fig. 4b. The hologram which has a size of about 3/4" by 3/4" is illuminated by the expanded laser beam. A fraction of the beam passes straight through the hologram and forms the zero-order image on the photographic plate or film. A second part of the beam is deflected by the holographic interference pattern off-axis and forms the real image on the plate. A third fraction is deflected into a direction on the other side of the axis and forms a beam which gives the impression to originate at the original object and thus carries the virtual image. Additional parts of the beam are deflected by the higher-order distributions and form the ghost images. Movable masks with rectangular cutouts are used to make several holograms and several reconstructed images on one plate.

Experimental Procedure

As a first step, a series of holograms was made of a line object on 649-F plates at a development time of five minutes by the use of the described setup. The light intensities of the reference and signal beams were carefully adjusted to correspond to a series of operational points along the T&E curve shown in Fig. 1. Six holograms were made on one plate. The intensity level of the reference beam was adjusted by inserting attenuators of varying attenuation such that six average levels of transmittance were obtained ranging from about .8 to .1 transmittance. The intensity of the signal beam was adjusted to correspond to amplitude level of $A \simeq 100$ (amplitude of sinusoidal variation of exposure) and kept constant when the six holograms were made. A similar set of holograms on one plate was made after substitution of a spherical lens for the cylindrical one. The focal region of the lens then represents a point source.

The reconstruction was made by illuminating the holograms by an expanded collimated laser beam and by photographing the real images on polaroid film. Three pictures were ually taken on one frame bymoving an opaque screen with a rectangular cut-out up and down in front of the polaroid film holder. The distance between hologram and film holder was adjustable to permit positioning of the film holder in the planes of the first and higher-order images of the line and point object.

Results

The first experiment was made to show first-order and higher-order images of a line source. Herewith, one hologram was used for reconstruction and the real images photographed three times in a row with the polaroid film holder placed at three distances. The positions coincided with the image planes of the original object (line source) and of the second-order and third-order ghost images. The three pictures are shown in Fig. 5. The upper picture shows a circular illuminated region in the center which represents the zero-order circular beam transmitted straight through the circular hologram. On the right-hand side is the image of the original line object. The distance between film and hologram was D_1 which is equal to that between object and the holographic plate when the hologram was made. The shadow on the left-hand side is caused by the beam which, if observed with the eye, would yield the virtual image.

The center picture below shows the second-order ghost image of the line object on the right-hand side. The distance between film and hologram was reduced to about one-half of that when the previous picture was taken. This distance is obtained by Eq. (37). It is observed that the lateral distance between image and axis is the same as before. This confirms the result of the theoretical analysis, Eq. (38). The eliptical image between the center zero-order image and the second-order line image is the result of the first-order beam which,

if continuing behind the plane of the film, would focus in the image of the original line object photographed in the preceding picture above.

When the lower picture was made, the film holder was moved upwards and placed at about $D_1/3$ from the hologram. In this plane, the beam resulting from the third-order nonlinearities becomes focused and forms a ghost image of the line object. It can be noted that the lateral distance from the axis of this image is somewhat smaller than in the preceding case. The elliptical images at the left of the line image are the result of the first and second order beams. It is observed that the light intensities of the reconstructed line images considerably decrease with increasing order number. The corresponding light amplitudes are proportional to the individual Chebyshev coefficients for the specific light levels when the hologram was made.

The purpose of the second experiment was the study of the influence of the bias level of the reference beam on the nonlinearities. The intensities of the second-order ghost images were compared at various amplitude levels of the reference beam. The amplitude of the signal beam was kept constant as indicated in the description of the experimental procedure in section B. The hologram was that of a line object. Figure 6 shows the results. Photographs were made on polaroid film of the real images of three holograms by moving the film holder up and down. The pictures were taken with the film plane in the image plane for the second-order ghost images. The ghost

images are focused in this plane and have the form of the original line object. The line images are shown on the right-hand side. The beams for the linear real and virtual images of the line object cause the elliptical images on both sides of the centrally located zero-order image.

In the upper picture, the light level of the reference beam was in the region for minimum noise-to-signal ratio (NSR) causing a transmittance of about .5 and giving minimum nonlinearities. The ghost image is rather weak. The lower picture shows the reconstructed images when the level was adjusted for a transmittance of about .15 giving a maximum NSR and hence large nonlinear effects. Correspondingly the intensity of the ghost image is rather strong. The picture in the center corresponds to an operational point on the T&E curve between the maximum and minimum at a transmittance of about .3 (see Fig. 1). At the reconstruction, the light level of the first-order beam was kept constant.

In the third experiment, the cylindrical lens was replaced by a spherical lens which formed a point source in the focal region. The resulting interference pattern is a hologram of a point object. Reconstruction in a slightly expanding beam resulted in the three photographs shown in Fig. 7. The upper photograph shows the reconstructed real image in the plane of the linear image where the right-hand illuminated point represents the image of the original object. The circular illuminated region in the center is the image resulting from the zero-order, straight-through beam. The two photographs below show the ghost images

caused by the second-order and third-order nonlinearities. The circular images between the point images on the right-hand side and the zero-order images in the center are the result of illumination by the lower-order beams. Light shadows left of center are the result of beams carrying the virtual image.

Conclusions

It was shown that relationships can be derived by the use of Chebyshev polynomials which describe the nonlinear effects in holographic processes. Equations were found for the transmittance of thin off-axis holograms of general, two-dimensional objects and for the reconstructed images in the Fresnel zone. The equations are complicated for general objects, as is the case at using other methods of representing nonlinear characteristics, such as Taylor series. The equations, however, become manageable for fundamental objects, particularly for line objects where the problem is one-dimensional. The results can be readily interpreted and were confirmed by experiments.

The equations and corresponding experiments confirm the previously reported observations that the nonlinear effects cause secondary or "ghost" images. The use of Chebyshev polynomials for the description of nonlinear characteristics offers the advantage that in the case of fundamental objects, the description of the transmittance distribution of the hologram becomes rather simple. Each term of the Chebyshev series directly represents a pair of ghost images. This is not the case if other methods of describing nonlinearities are used. Infinite series are then

obtained instead of single terms. If the hologram is illuminated by coherent light, the elementary harmonic distributions which superimposed represent the transmittance and which are described by the various Chebyshev coefficients deflect fractions of the beam passing through the hologram. The fractional beams are focused at different positions and form the images. The described experiments follow instructively the derived equations as shown by the reproduced photographs of the real image in Figs. 5 through 7.

Another merit of the new method is the fact that the nonlinear effects can be treated numerically. Using Chebyshev polynomials, the various coefficients of the series represent pairs of ghost images. Hence, the light power carried in the beams forming the various images actually can be computed. Ratios for the light powers forming the various ghost images to that of the actual linear image can be found. This permits determination of individual noise-to-signal ratios and a corresponding over-all ratio. The latter represents the ratio of the light power forming all ghost images to that of the linear image of the original object. Hence, one can find figures of merit for the quality of holographic reproduction with regard to nonlinearities. This in turn opens the way for the numerical evaluation and comparison of film, plate, and other recording material for holography and of the related processing methods. It also permits determination of optimum operational conditions given by the ratio of the level of the signal beam to that of

the reference beam. The new method thus seems to have a number of merits, however, further studies and further use will give an indication of their importance.

References

1. A. Kozma, J. Opt. Soc. Am. 56, 428 (1966).
2. A. A. Friesem, A. Kozma, and G. F. Adams, Appl. Opt. 6, 851 (1967).
3. A. A. Friesem and J. S. Zelenka, Appl. Opt. 6, 1755 (1967).
4. H. J. Gerritsen, E. G. Ramberg, and S. Freeman, Image Processing with Nonlinear Optics (Symposium on Modern Optics, Polytechnic Institute, Brooklyn, 1967).
5. O. Bryngdahl and A. Lohmann, Nonlinear Effects in Holography [IBM Research Report RJ 491 (#10467), April, 1968].
6. J. W. Goodman and G. R. Knight, J. Opt. Soc. Am. 58, 1276 (1968).
7. J. P. Moffatt, Effects of Geometric Deviations and Nonlinearities in Coherent Optical Data Processors (Ph.D. Dissertation, North Carolina State University, Raleigh, North Carolina, 1968).
8. David Middleton, An Introduction to Statistical Communication Theory (McGraw Hill Book Company, New York, 1960).
9. M. Born and E. Wolf, Principles of Optics (Pergamon Press, London, 1965), Third Edition, p. 380.

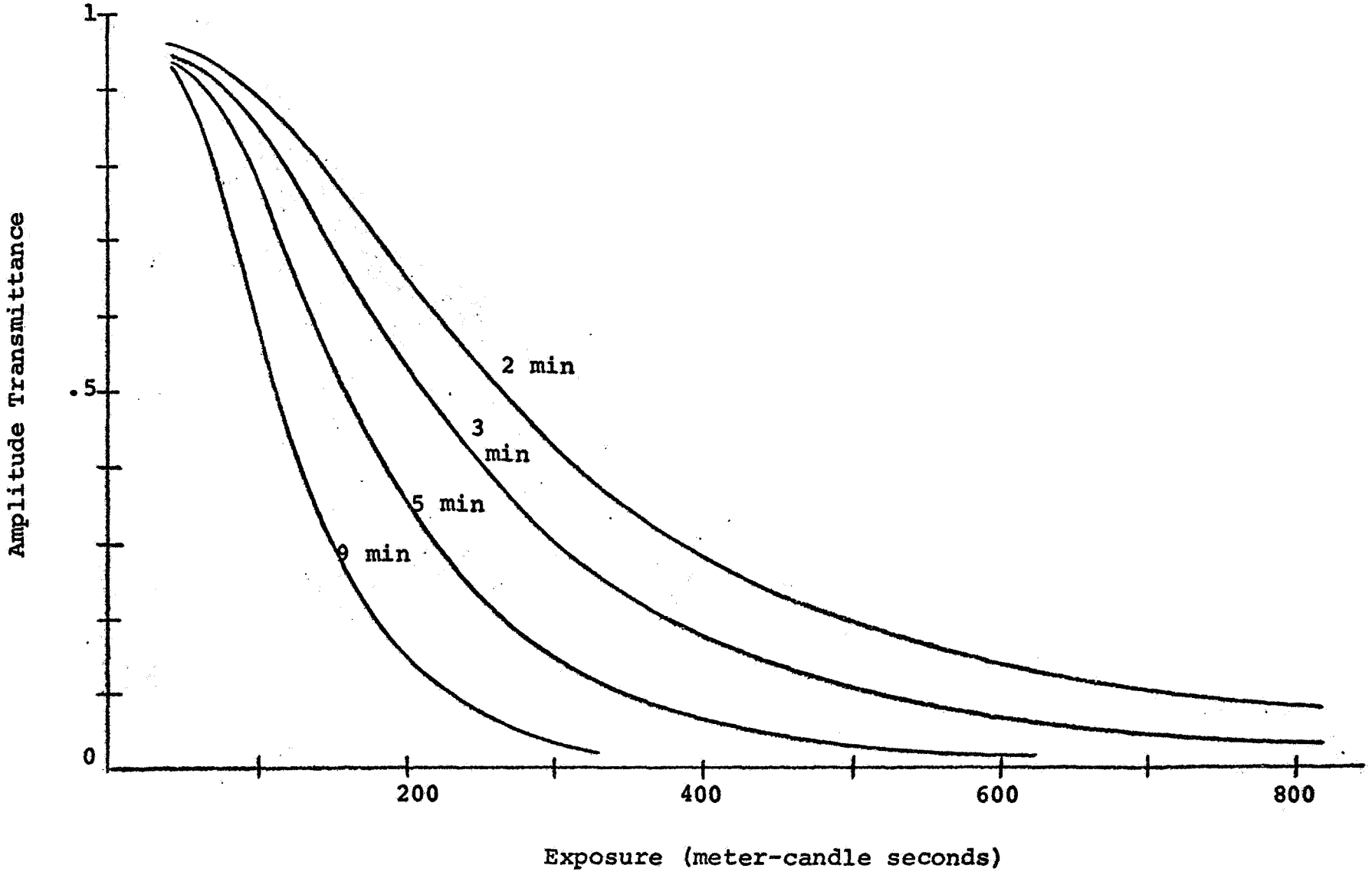

Fig. 1 Characteristic T&E curve (transmittance-versus-exposure) for 649-F Spectroscopic plates

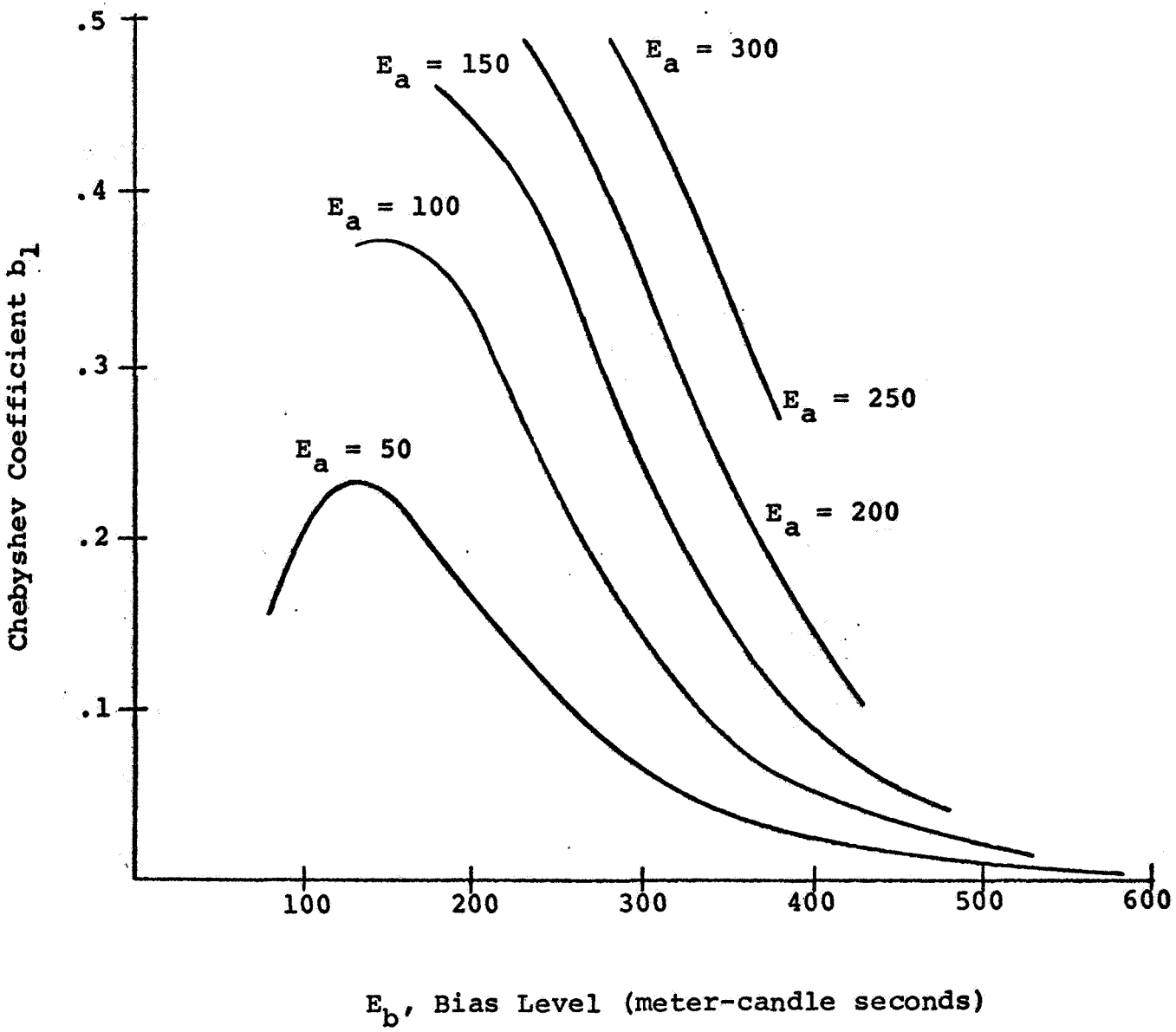

Fig. 2 Chebyshev coefficient b_1 as a function of bias level E_b and exposure amplitude E_a.

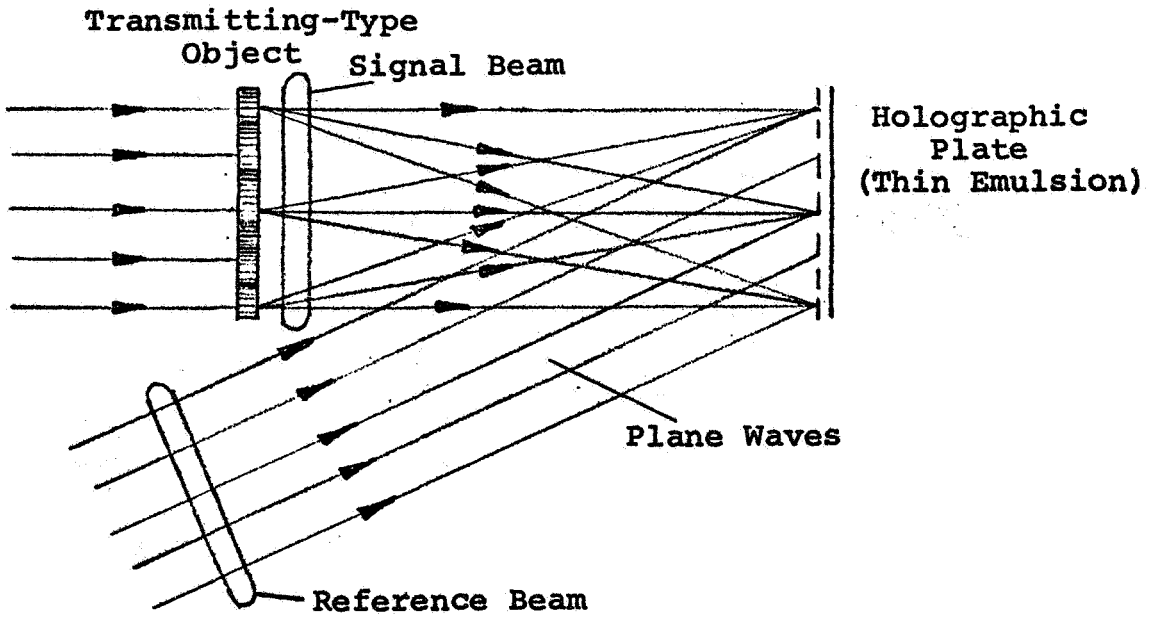

Fig. 3 Beam geometry at holography
(Fresnel hologram)

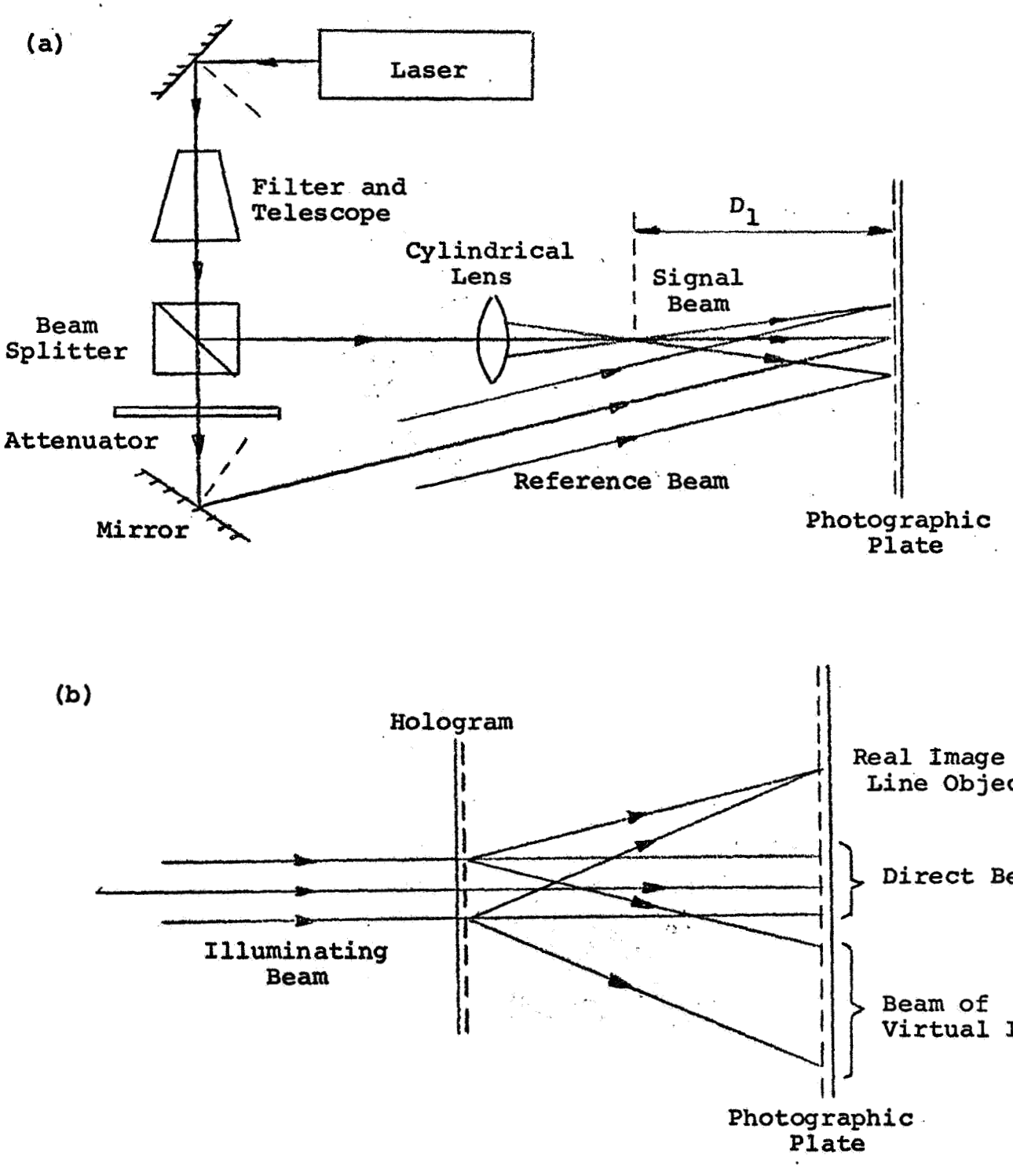

Fig. 4 Holography of a line object

a. Setup for making the hologram
b. Reconstruction and image geometry

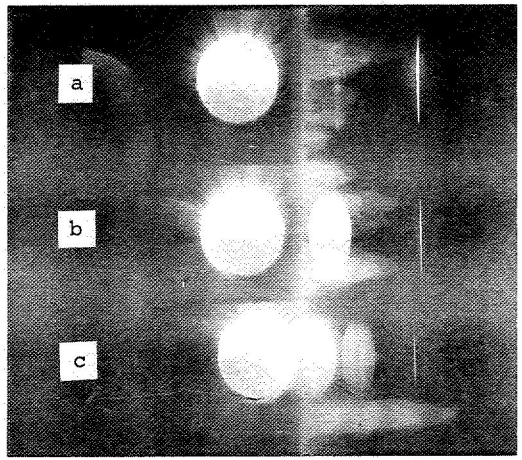

Fig. 5

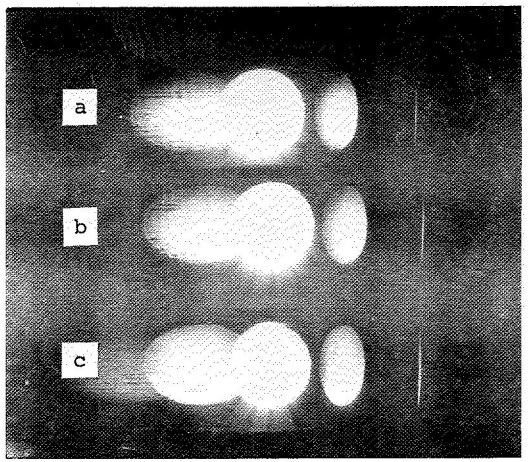

Fig. 6

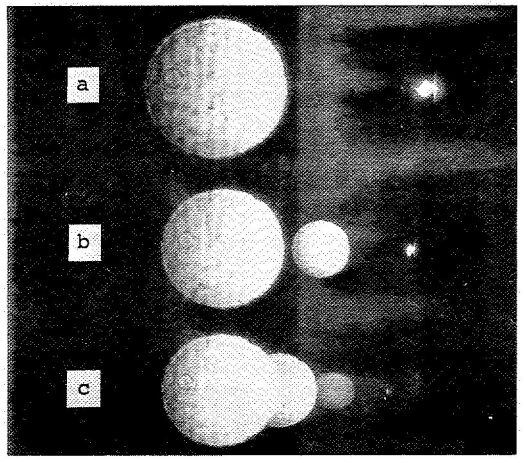

Fig. 7

Fig. 5 Real images of a line object.
a. Image of actual object (first-order image).
b. Second-order ghost image.
c. Third-order ghost image.

Fig. 6 Effects of the bias exposure (light level of the reference beam) on the intensity of ghost images.
a. Low bias level.
b. Medium level.
c. High level.

Fig. 7 Real reconstructed images of a point object. (Reconstruction in slightly expanding beam.)
a. Image of object.
b, c. Second and third-order ghost images.